Electronic Supplementary Material (ESI) for Nanoscale.

Biomass-Derived Carbonaceous Positive Electrodes for Sustainable Lithium-Ion Storage

Tianyuan Liu,[a] *Reza Kavian,*[a] *Zhongming Chen,*[b] *Samuel S Cruz,*[a] *Suguru Noda,*[b] *Seung Woo Lee*[a,*]

a. George W. Woodruff School of Mechanical Engineering, Georgia Institute of Technology Atlanta, Georgia 30332, United States

b. Department of Applied Chemistry, Waseda University, 3-4-1 Okubo, Shinjuku-ku, Tokyo 169-8555, Japan

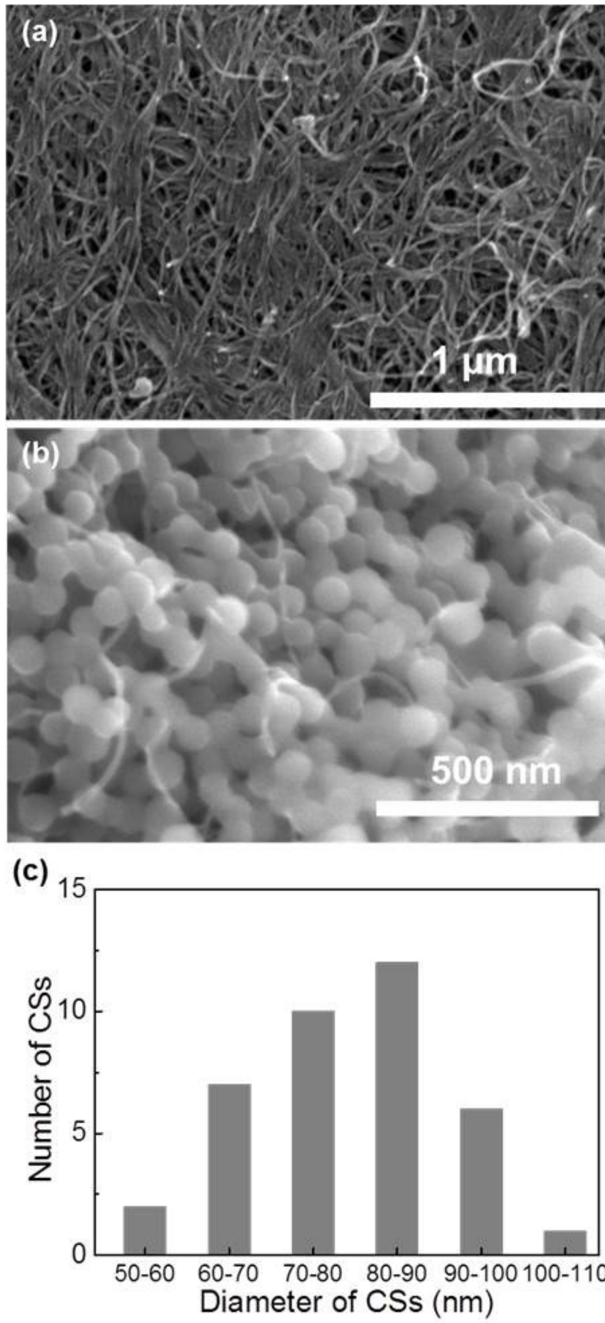

Figure S1. SEM images of (a) the pristine few-walled carbon nanotube (FWNT) film after the microwave process and (b) the composite film including 68 wt% of carbon spheres (CS-0.68). (c) A histogram of the diameter of the carbon spheres, which was analyzed by SEM. The average diameter is 79.9±11.9 nm by counting 38 carbon spheres.

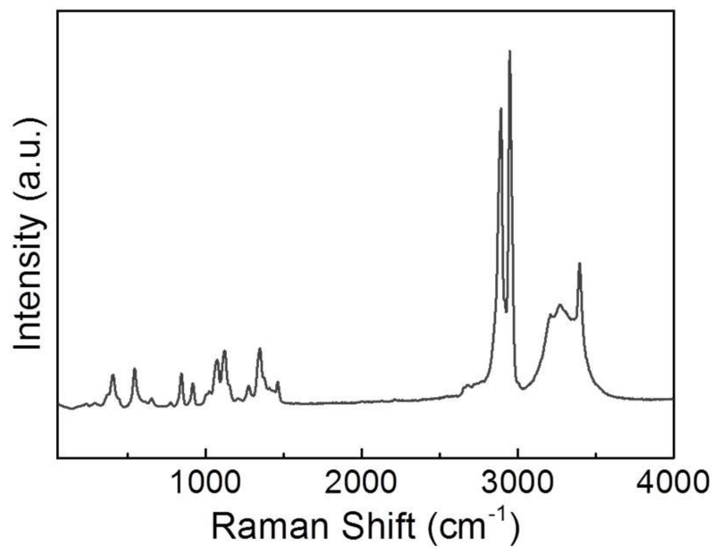

Figure S2. (a) Raman spectrum of glucose in the range of 50-4000 cm^{-1}. A broad plateau between 3100 and 3500 cm^{-1} is associated with bonded hydroxyl groups, while superimposed three sharp peaks above 3200 cm^{-1} are ascribed to non-hydrogen-bonded hydroxyl groups.[1] Two sharp peaks between 2800 and 3000 cm^{-1} can be assigned to C-H symmetric and asymmetric stretching.[1] A complex series of sharp peaks below 1200 cm^{-1} are due to the vibration of the C-O, C-C, and C-O-H groups [1]

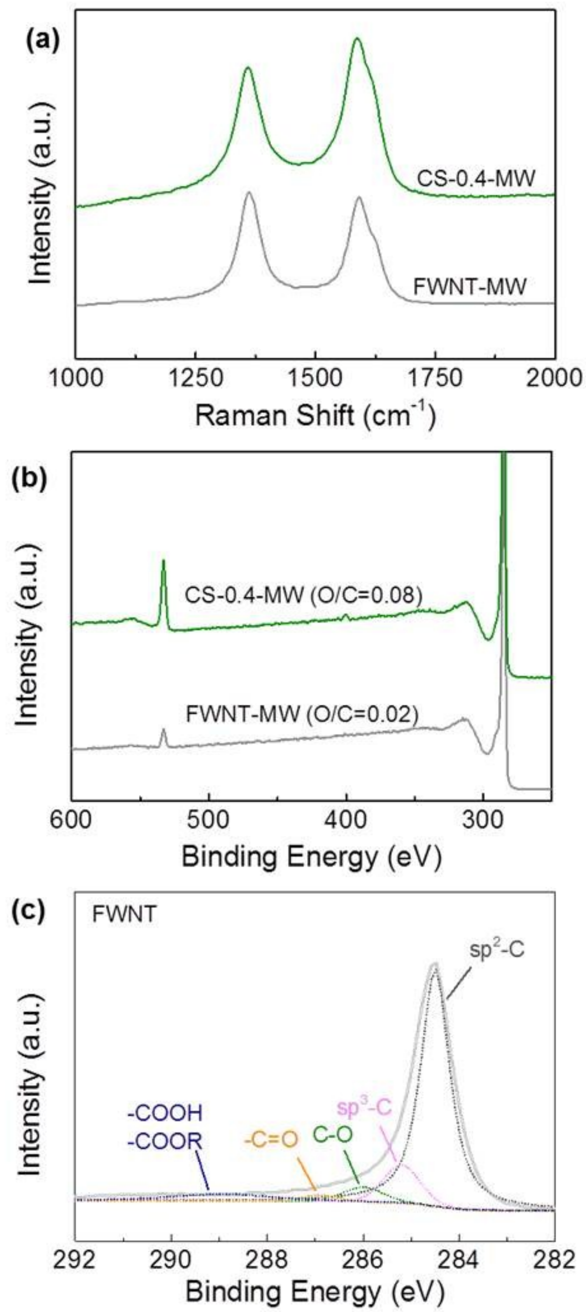

Figure S3. (a) Raman spectra, (b) X-ray photoelectron spectroscopy (XPS) wide scan survey of the micorwave processed FWNT film and the CS-0.4-MW. (c) High resolution C1s spectra of pristine FWNTs.

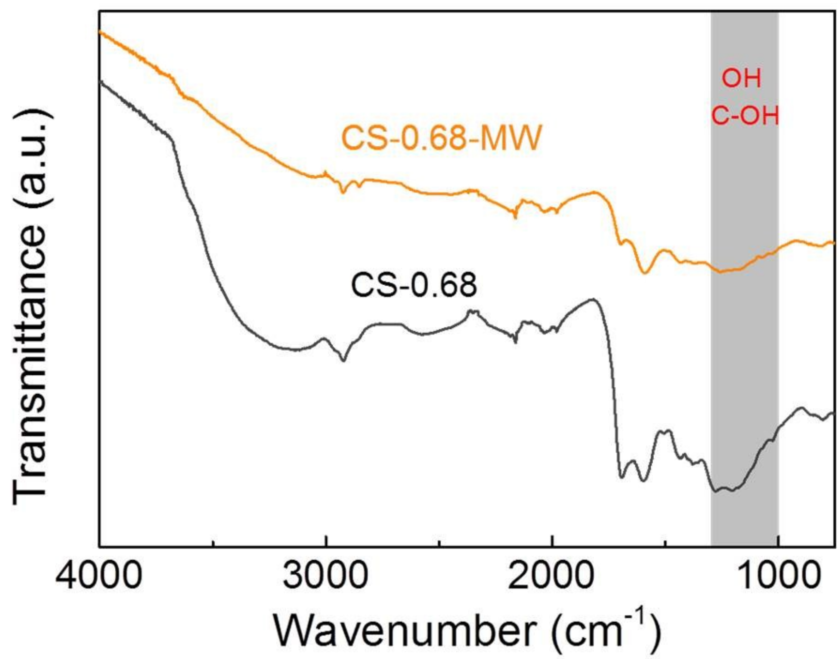

Figure S4. (a) Fourier transform infrared (FTIR) spectroscopy comparison of the composite films before (CS-0.68) and after (CS-0.68-MW) microwave process.

Table S1. Densities and electrical conductivities of the pristine FWNT and composite films.

Sample	**Density (g/cm^3)**	**Electrical Conductivity (Scm^2/g)**
FWNT	0.24	209.2
FWNT-MW	0.20	183
CS-0.4	0.37	93
CS-0.4-MW	0.34	93.8
CS-0.68	0.41	64.4
CS-0.68-MW	0.35	75.7

Table S2. Capacity comparison of various carbon based positive electrodes.

Sample	**Voltage Window (V)**	**Capacity (mAh/g)**	**Reference**
Activated Carbon	3.05 - 4.3 V	38.4	*J. Power Sources* **2015,** 282, 385-393
Activated Carbon	3 - 4.6 V	5 - 71	*Sci. Rep.* **2013**, 3, 3002
Oxidized FWNT	1.5 – 4.5 V	87 – 118	*Energy Environ. Sci.,* **2012**, 5, 5437-5444
Reduced Graphene Oxide (rGO)	1.5-4.5	125	*ACS Appl. Mater. Interfaces 2013, 5,*
Multi-walled carbon nanotube+rGO	1.5 – 4.5 V	110-135	*Adv. Funct. Mater.* **2013**, 23, 1037–1045
folded-graphene film (*f*GF)	1.5 – 4.5 V	160	*Chem. Mater.*, **2015**, 27, 3291–3298
Functionalized Graphene	1.5 – 4.5 V	102 - 165	*J. Phys. Chem. Lett.* **2014**, 5, 4324–4330

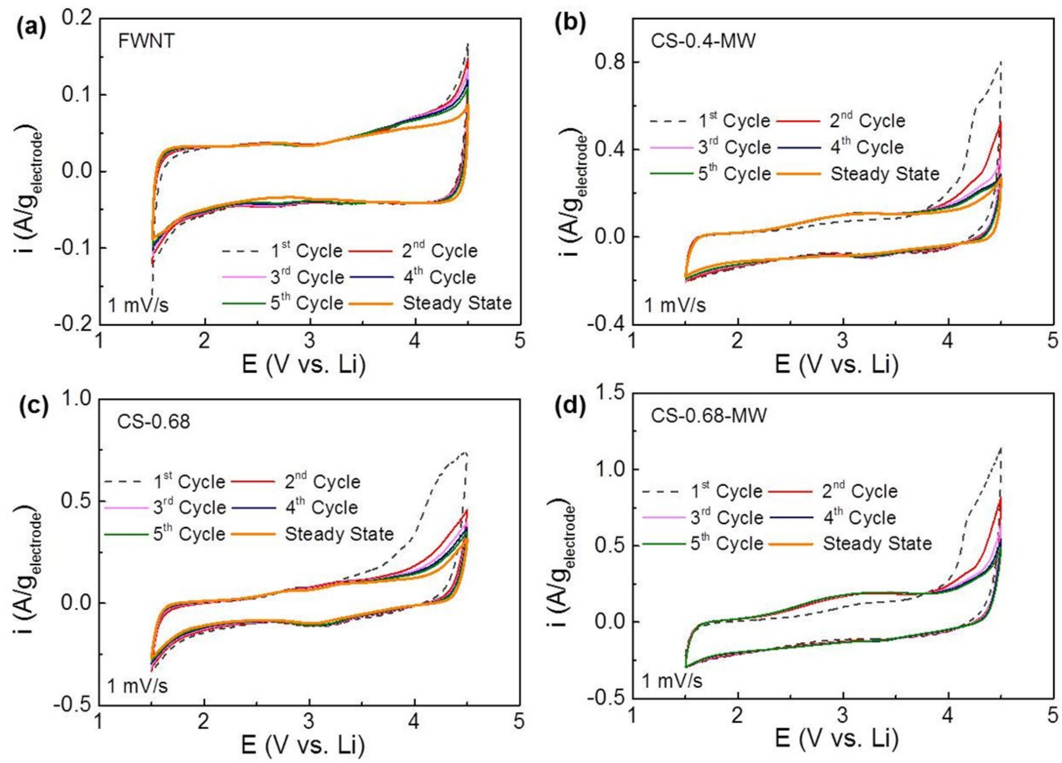

Figure S5. CV scans of (a) the pristine FWNTs electrode, (b) CS-0.4-MW, (c) CS-0.68, and (d) CS-0.68-MW as a function of cycle number.

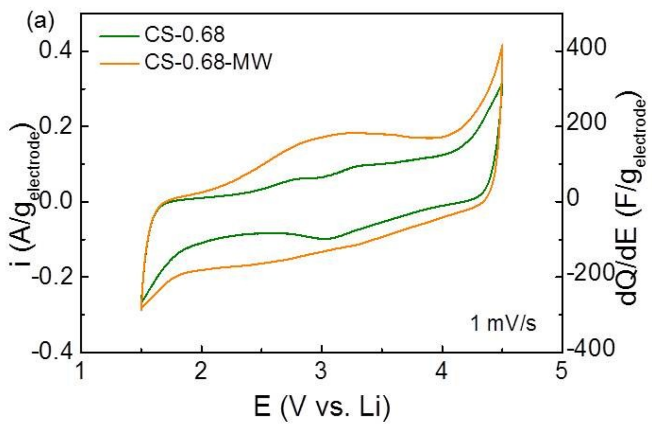

Figure S6. Comparison of steady state CV scans before (CS-0.68, olive) and after (CS-0.68-MW, orange) microwave process at (a) 1 mV/s and (b) 100 mV/s. A CV scan of the FWNT electrode was compared as control at Figure S6b.

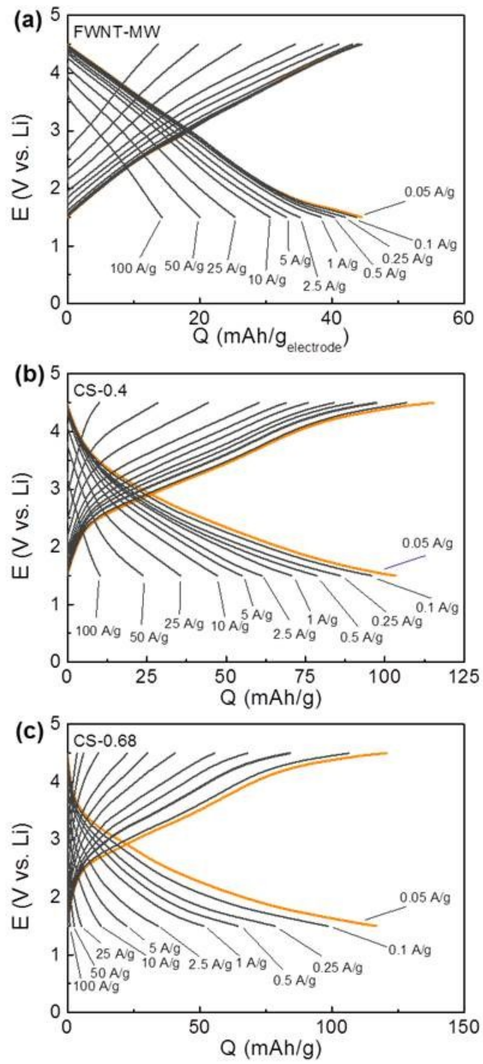

Figure S7. Rate-dependent galvanostatic charge and discharge curves for (a) the microwave processed FWNT film (FWNT-MW), (b) CS-0.4, and (c) CS-0.68 in lithium cells.

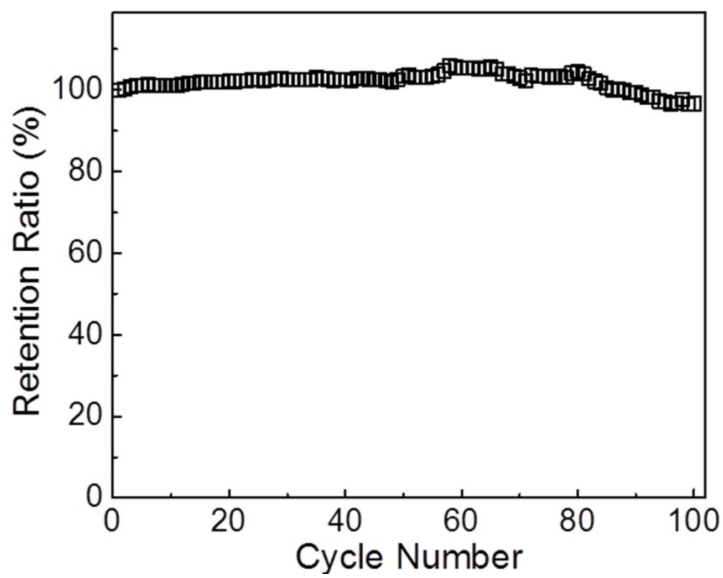

Figure S8. Cycling stability of CS-0.68-MW at a current density of 0.1 A/g up to 100 cycles.

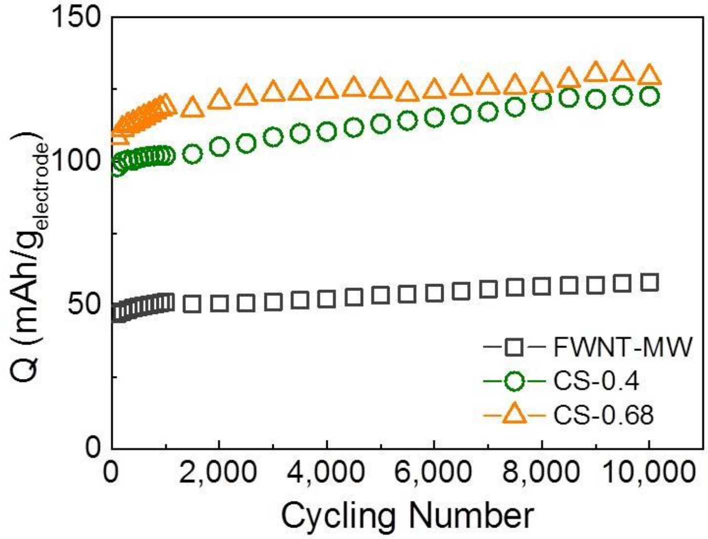

Figure S9. Specific capacities of the FWNT-MW, CS-0.4 and CS-0.68 as a function of cycle number up to 10,000 cycles using an accelerating cycling method. Data points indicate specific discharge capacities of the films measured at a slow rate of 0.1 A/g. Between each slow measurement, the cells were cycled at high current density of 10 A/g.

References:

1. http://www.mccroneatlas.com/viewer/text.asp?IMAGE_ID=231417&PARTICLE_ID=71&TECHNIQUE_ID=5&MODE=RAMAN.